VI International Conference on Computational Methods for Coupled Problems in Science and Engineering
COUPLED PROBLEMS 2015
B. Schrefler, E. Oñate and M. Papadrakakis (Eds)

A MAGNETO-THERMO-METALLURGICAL FINITE ELEMENT MODEL APPLIED TO INDUCTION HARDENING PROCESSES

MATTIA SPEZZAPRIA, MICHELE FORZAN AND FABRIZIO DUGHIERO

Laboratory of Electroheat (LEP) - Department of Industrial Engineering (DII)
University of Padova
Via Gradeniglo 6/a, 35131 Padova, Italy
e-mail: mattia.spezzapria@dii.unipd.it, web page: http://www.dii.unipd.it

Key words: Induction Hardening, Multiphysics, Phase transformation, Quenching

Abstract. Induction hardening has been widely applied for the heat treatment of components mainly in the aeronautical and automotive sectors because of its peculiar advantages like high quality and repeatability of process and its easy automation. A multi-scale multiphysical finite element (FE) analysis is presented in this paper for the prediction of microstructural evolution during induction hardening processes. An ad hoc external routine has been developed in order to calculate the phase changes during heating and cooling process associated with non-isothermal transformations. This routine has been coupled with commercial FEM codes able to solve the coupled electromagnetic and thermal problem that typically describes the induction heating processes. During the heating, the magnetic field generated by the coil induces currents in the workpiece and as consequence the heating of conductive material by Joule effect.
Material properties depend on the temperature distribution but also on the microstructure since the material could be seen as a mixture of different phases, each one with different physical properties. The effect of latent heat of solid-solid phase transformations has been also considered.
From the solution of the coupled steady-state, at a given frequency, electromagnetic and transient thermal problem, temperature distribution as well as heating and cooling rates are used for the evaluation of the existing metallurgical phases at every time step.

1 INTRODUCTION

Heat treatments have been traditionally used in order to improve the mechanical properties of steel parts. In the particular case, superficial heat treatments permit to modify only the external layer of a work-piece, maintaining unchanged the core of the material. Nowadays Contour Induction Hardening (CIH) process is increasingly applied instead of carburizing process, due to its repeatability and easy automation.

During induction hardening, the magnetic field generated by a coil induces current in the work-piece, which is heated by Joule effect. Thermal history induces, during the process, a solid-solid phase transformation in the material.

Due to its multiphysical nature, simulation tools become essential for the prediction of phase transformations.

Many studies have been carried out in the field of heating by induction [1, 2, 3, 4] and in

the specific case of induction hardening [5, 6, 7], but the multiphysical simulation of all the phenomena that occur during the whole process is still an open task.

Several models for the simulation of quenching have been proposed in the past [8, 9, 10, 11, 12, 13], but in the most of cases the body was uniformly heated above the austenitization temperature. In induction hardening, temperature distribution exhibits steep gradients and the actual distribution of austenitization in the piece is not uniform.

In other hand many authors proposed different models for the simulation of laser welding process [14, 15, 16], that can be considered, for some aspects (phase transformations, high heating rate), similar to induction hardening.

2 ELECTROMAGNETIC AND THERMAL FORMULATION

The mathematical analysis of coupled electromagnetic and thermal problem has been carried out by solving Maxwell and Fourier equations. The computation of magnetic flux density and induced current density is obtained by solving a time-harmonic eddy-current problem at a prescribed frequency.

The numerical solution of the EM problem has been carried out by applying the well-known Magnetic Vector Potential formulation where the Coulomb gauge has been imposed in order to guarantee the uniqueness of magnetic vector potential $\boldsymbol{A}$.

In the conductive region Faraday-Neumann law equation implies the existence of an electric scalar potential V, such that [2, 17]

$$\boldsymbol{E} = -j\omega\boldsymbol{A} - \nabla V \tag{1}$$

where $\boldsymbol{E}$ is the electric field and ω the angular frequency. Given that induced current density $\boldsymbol{J}$ can be written as:

$$\boldsymbol{J} = -\sigma(j\omega\boldsymbol{A} + \nabla V) \tag{2}$$

in which σ is the electrical conductivity of the material. The previous relations and Maxwell equations lead to the following system of equations:

$$\begin{cases} \nabla \times \left(\frac{1}{\mu}\nabla \times \boldsymbol{A}\right) + \sigma(j\omega\boldsymbol{A} + \nabla V) = 0 & (3) \\ \nabla \cdot \sigma(j\omega\boldsymbol{A} + \nabla V) = 0 & (4) \end{cases}$$

When the current density distribution is known in the conductive body, the distribution of power densities by Joule effect can be evaluated as follow:

$$w_p = \rho|J|^2 = \rho\omega^2|A|^2 \tag{5}$$

where ρ is the electrical resistivity.

The power densities calculated in the electromagnetic step are used as internal power densities in the transient thermal simulation and the thermal problem has been solved by means of Fourier equation for heat conduction:

$$\nabla(\lambda\nabla T) + w_p = \gamma C_p \frac{dT}{dt} \tag{6}$$

in which γ is the density and C_p the specific heat.

The thermal exchange by convection and radiarion have been taken into account during the heating stage on the surfaces of contact between the trated body and the air:

$$\Phi(T_S, T_\infty) = h(T_S - T_\infty) + k_B \varepsilon \left({T_S}^4 - {T_\infty}^4\right) \tag{7}$$

where h is the coefficient of heat exchange by convection, k_B the Stephan-Boltzmann constant and ε the emissivity of the surface. The temperature distribution calculated has been used for updating the electromagnetic properties in order to calculate accurately the Joule losses distribution for every time step of thermal transient simulation.

3 THERMO-METALLURGICAL FORMULATION

The nodal power densities calculated in the EM step for each time step are the internal heat sources in a coupled thermo-metallurgical model.

In the thermo-metallurgical model the material can be described as a mixture of different phases, each one with different physical properties. The global material properties can be extimated through a linear rule of mixture[8,9]:

$$P(T, \xi_k) = \sum_{k=1}^{N} P_k(T) \xi_k \tag{8}$$

where $P_k(T)$ is the value of the physical property, temperature dependent and ξ_k is the volume fraction of the k-th phase. During phase transformations latent heat is absorbed or released by the body and this effect mustbe included in the calculations for an accurate extimation of temperature distribution. The temperature distribution within the workpiece is determined by the modified heat conduction equation:

$$\nabla(\lambda \nabla T) + w_p + \sum_{k=1}^{N} \Delta H_k \frac{d\xi_k}{dT} = \gamma C_p \frac{dT}{dt} \tag{9}$$

where ΔH_k is the enthalpy change due to phase tranformation.

3.1 Austenitization

During the induction heating the initial microstructure (generally made of pearlite, ferrite and carbides) transforms when austenitization temperatures are reached: below the Ac1 temperature the microstructure is composed by ferrite and pearlite, between Ac1 and Ac3 it is a mixture of ferrite, pearlite and austenite and above Ac3 the microstructure is typically inhomogeneous austenite. These temperature are affected by the chemical composition, heating rate and also by the microstructure. The kinetics of transformation during high heating rate processes can be calculated through the use of Continous Heating Transformation (CHT) Diagrams, which provide an indication of the transformation temperatures at different heating rates. In this study, the CHT diagram has been derived from the literature [18] and the austenite transformation kinetic has been simplified as follow:

$$\xi_A = \begin{cases} 0 & , \quad T < Ac_1(\dot{T}) \\ \dfrac{T - Ac_1(\dot{T})}{Ac_3(\dot{T}) - Ac_1(\dot{T})} & , \quad Ac_1(\dot{T}) \le T \le Ac_3(\dot{T}) \\ 1 & , \quad T > Ac_3(\dot{T}) \end{cases} \tag{10}$$

3.2 Quenching

During quenching several types of microstructures are generated by the decomposition of austenite (pearlite, ferrite, bainite and martensite), depending on the cooling rate.
The microstructure can be evaluated starting from the thermal history using Isothermal (IT) diagrams. These diagrams can be drawn through a numerical method developed by Kirkaldy [19] and reviewed by Victor Li [20] derived from Zener [21] and Hillert [22] formulas, based on kinetic-chemical equations:

$$\tau(X,T) = \frac{F(C,Mn,Si,Ni,Cr,Mo,G)}{\Delta T^n \exp\left(-\frac{Q}{RT}\right)} S(X) \tag{11}$$

in which τ is the time needed to transform, X the chemical composition, T the temperature, ΔT the undercooling, Q the activation energy, R the gas constant, and n is an empirical constant dependent on the diffusion mechanism (n=2 for volume and n=3 for boundary diffusion). S(X) is the reaction term defined by Kirkaldy, which approximates the sigmoidal effect of phase transformation:

$$S(X) = \int_0^X \frac{dX}{X^{0.4(1-X)}(1-X)^{0.4X}} \tag{12}$$

Considering the study carried out by Victor Li in [20], a reasonable value of the activation energy for all diffusional transformation is 27500 Kcal/(mol °C)
The time of transformation for a fixed temperature can be found through the following expressions:

$$\tau_F = \frac{\exp(-4.25 + 4.12C + 4.36Mn + 0.44Si + 1.71Ni + 3.33Cr + 5.19\sqrt{Mo})}{2^{0.41G}(Ae_3 - T)^3 \exp\left(-\frac{27500}{RT}\right)} S(X) \tag{13}$$

$$\tau_P = \frac{\exp(1 + 6.31C + 1.78Mn + 0.31Si + 1.12Ni + 2.70Cr + 4.06Mo)}{2^{0.32G}(Ae_1 - T)^3 \exp\left(-\frac{27500}{RT}\right)} S(X) \tag{14}$$

$$\tau_B = \frac{\exp(-10.23 + 10.18 + 0.85Mn + 0.55Ni + 0.90Cr + 0.36Mo)}{2^{0.29G}(B_S - T)^2 \exp\left(-\frac{27500}{RT}\right)} S(X) \tag{15}$$

Respectively for ferrite, pearlite and bainite transformation.

The transformation temperatures have been calculated through the following models:

$$Ae_3 = 883.49 - 275.89C + 90.91C^2 - 12.26Cr + 16.45CCr - 29.96CMn + 8.49Mo + \\ -10.8CMo - 25.56Ni + 1.45MnNi + 0.76Ni^2 + 13.53Si - 3.47MnSi \tag{16}$$

$$Ae_1 = 739 - 22.8C - 6.38Mn + 18.2Si + 11.7Cr - 15Ni - 6.4Mo - 5V - 20Cu \tag{17}$$

$$B_S = 637 - 58C - 35Mn - 15Ni - 34Cr - 41Mo \tag{18}$$

$$M_S = 539 - 423C - 30.4Mn - 17.7Ni - 12.1Cr - 7.5Mo + 10Co - 7.5Si \tag{19}$$

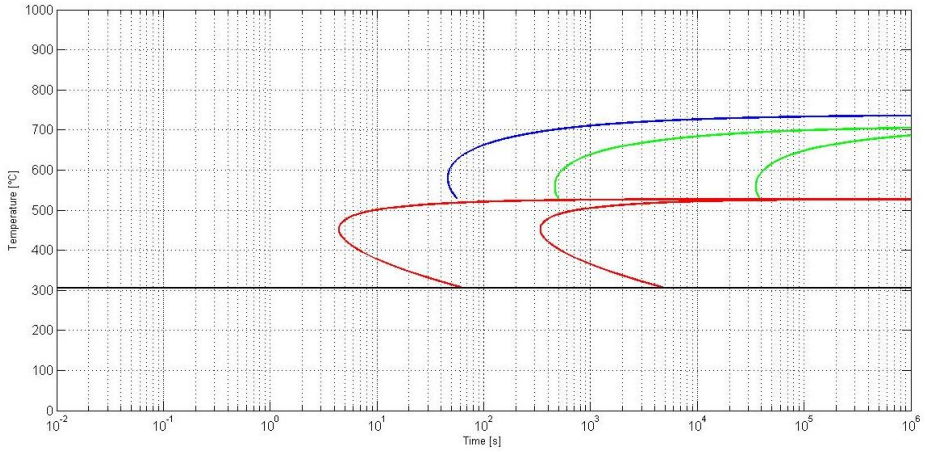

Figure 1: Calculated TTT Diagram for AISI4340

Once the IT diagram have been calculated, an analytical procedure has been developed for the calculation of microstructure evolution during quenching. Considering isothermal conditions, the kinetics of diffusional transformation can be expressed through the Johnson-Mehl-Avrami-Kolmogorov (JMAK) equation:

$$\xi_k = 1 - \exp(-b_k t^{n_k}) \tag{20}$$

where ξ_k is the total ammount of transformed phase, t is the time, b_k and n_k coefficients directly deduced from IT diagram.
Diffusive transformations always require an incubation time before starting and this can be explained through Sheil's additivity rule:

$$S = \sum_{i=1}^{n} \frac{\Delta t_i}{\tau_s(t_i)} = 1 \tag{21}$$

in which $\tau_s(t_i)$ is the incubation time at a current temperature and Δt_i is the time increment. Transformation begins when Scheil's sum is equal to unity.

During quenching the material is never subjected to isothermal conditions and also sometimes the austenite is not the only one metallurgical phase existing in the material. To solve this problem the thermal history during the quenching needs to be discretized into isothermal steps. The effective elapsed time must be corrected, becouse of the different kinetics of transformation that occur during each step and can be calculated as the sum of the time step and a fictitious time evaluated from the IT diagrams[13]:

$$t_k^* = \left[\frac{-ln(-\xi_{k-1})}{b_k}\right]^{\frac{1}{n_k}} \tag{22}$$

where ξ_{k-1} is the transformed phase in the previous step. Once the fictitious time is known a fictitious volume fraction ξ_i^* can be calculated through the JMAK equation:

$$\xi_k^* = 1 - exp[b_k(t_k^* + \Delta t)^{n_k}] \tag{23}$$

Hence the practical transformad volume fraction is:

$$\xi_k = (\xi_{k-1}^A - \xi_{k-1})\xi_{max} \tag{24}$$

in which ξ_{k-1}^{A} and ξ_{k-1} are respectively the austenite volume fraction and the transformed phase in the previous step and ξ_{max} is the maximum possible transformed fraction.
The equation considers that a part of the whole microstructure may not transform becouse already transformed or not austenitized; this is the case of coexistence of different phases due to a partial austenitization that occurs where Ac3 temperature has not been reached.

A different formaulation is used to model the martensitic transformation that describe this process as a diffusionless (or displacive) transformation.

The martensite volume fraction is generally evaluated through the Koistinen-Marburger (KM) model [23], but it tends to underextimate the transformed part in low-alloy steels. In this model, the martensite volume fraction has been calculated through a semi-empirical model proposed by Lee [10]:

$$\xi_M = \xi_A \cdot \{1 - \exp[-K_{LV}(M_S - T)^{n_{LV}}]\} \tag{25}$$

in which ξ_M is the total ammount of martensite, ξ_A the volume of parent phase, K_{LV} and n_{LV} are two coefficients dependent by the chemical composition:

$$K_{LV} = 0.0231 - 0.0105C - 0.0017Ni + 0.0074Cr - 0.0193Mo \tag{26}$$

$$n_{LV} = 1.4304 - 1.1836C + 0.7527C^2 - 0.0258Ni - 0.0739Cr + 0.3108Mo \tag{27}$$

4 FE SIMULATION PROCEDURE AND INPUT DATA

In this study the multiphysical model has been applied to a 2D axy-symmetric geometry. The electromagnetic and thermal simulation for the determination of Joule losses distribution has been solved by means of the commercial FEM software Flux 2D [24].
A circular billett (r=10 mm, h=60 mm) has been heated by a rectangular section coil (15x5x1.5 mm) witha C-shaped flux concentrator. Flux concentrator are often used in induction heating for increasing the efficiency of the process and improving thecontrol of heating pattern.
The billet is made in AISI 4340, a low alloy steel, often used in aeronautical and automotive sectors due to its high mechanical properties and hardenability.

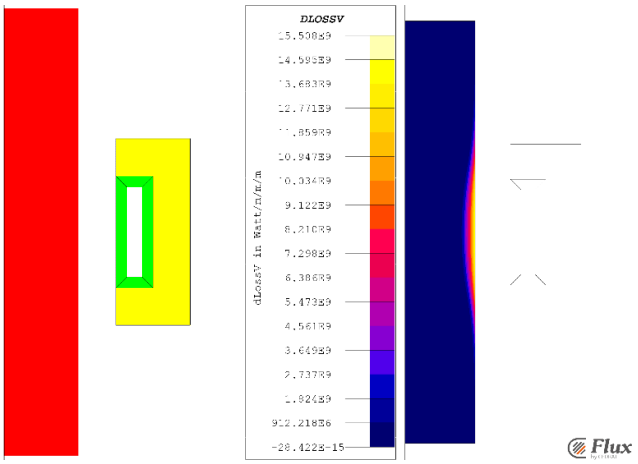

Figure 2: Geometry layout of the electromagnetic-thermal coupled simulation (left) and Joule losses distribution at the beginning of the heating process (right)

In this simulation the material of the billet has been considered as a unique phase with temperature dependent physiscal properties. An approximation of the effect of the latent heat absorbed during austenitic phase transformation have been introduced in the volumetric heat capacity.

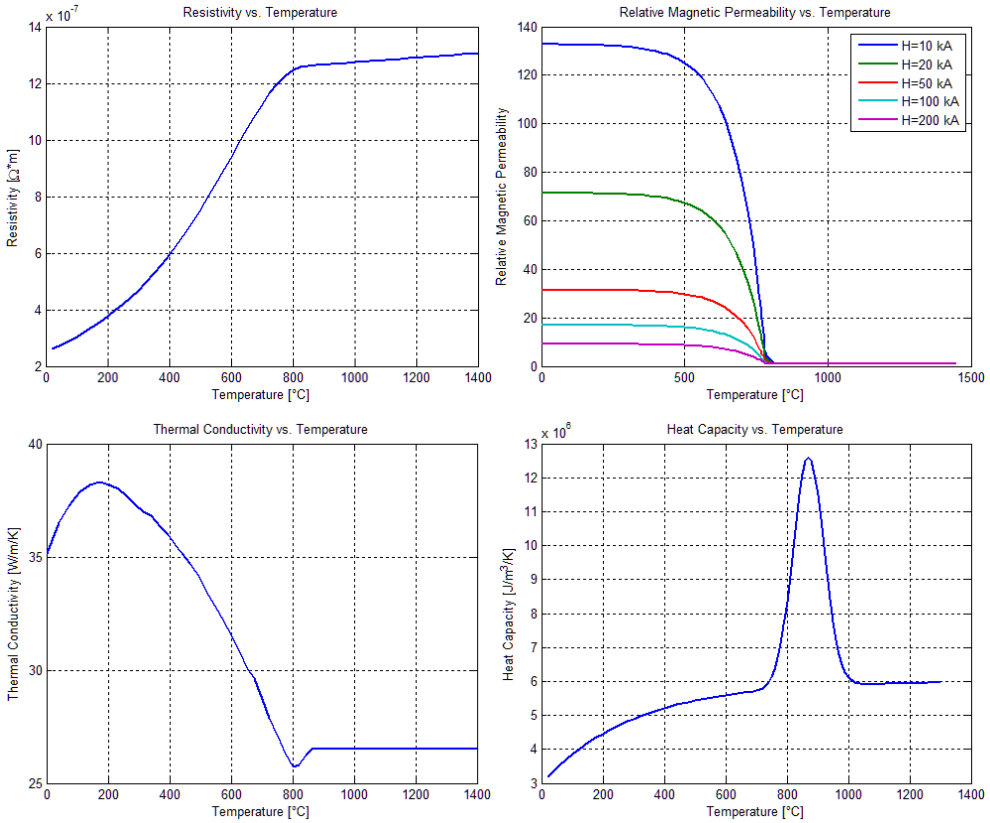

Figure 3: Physical properties of AISI 4340 - Resistivity (top-left), magnetic permeability (top-right), thermal conductivity (bottom-left) and volumetric heat capacity (bottom-right)

The heating process consists on a single shot step in wich the coil is fed by a current of 4300 A at 10 kHz for 1s. During heating the thermal losses by convection and radiation have been considered on the line that describes the external surface of the billet through a constant heat convection coefficient $\varepsilon = 15\ W/(m^2K)$ and a emissivity $\alpha = 0.8\ W/(m^2K^{-4})$.
At the end of electromagnetic-thermal coupled simulation developed in the commercial FEM code Flux2D, nodal power densities are exported at each time step to the thermo-metallurgical simualtion as internal power densities. The thermo-metallurgical simulation has been developed in Comsol with an ad hoc Matlab routine for the calculation of phase transformations.

In this model the material is modeled as a mixture of different phases,each one described by its specific material properties.

At the end of heating the billet is rapidly quenched with a acqueous polymer solution of polyalkilenglicole (PAG) at 12%. In order to simulate the strong temeprature variations of the quenching, a precise description of convective heat exchange parameter is mandatory. The mechanism of quenching is affected by many factors, which significantly influence the

performance of this process. In general, cooling occurs in three different stages: the early vapor phase, governed by convection and conduction through a vapor film around the work-piece; the main boiling phase, ruled by conduction between the hot surface and the quenchant, and the late convection phase into the liquid.

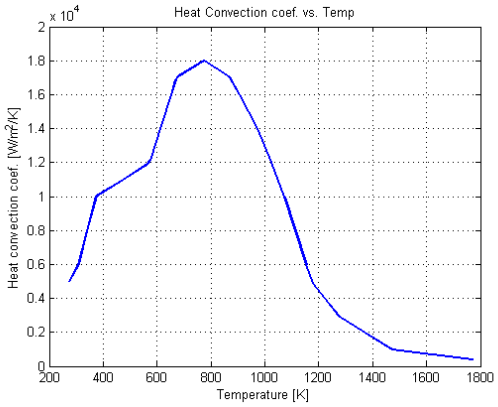

Figure 4: Convective heat exhange coefficient in function of the superficial temperature of the body

In figure 5 the martensite distribution at the end of quenching step is shown. In this type of calculation the effect of overtempering has not been taken into account insofar the tempering kinetics will be a subject of a further work.

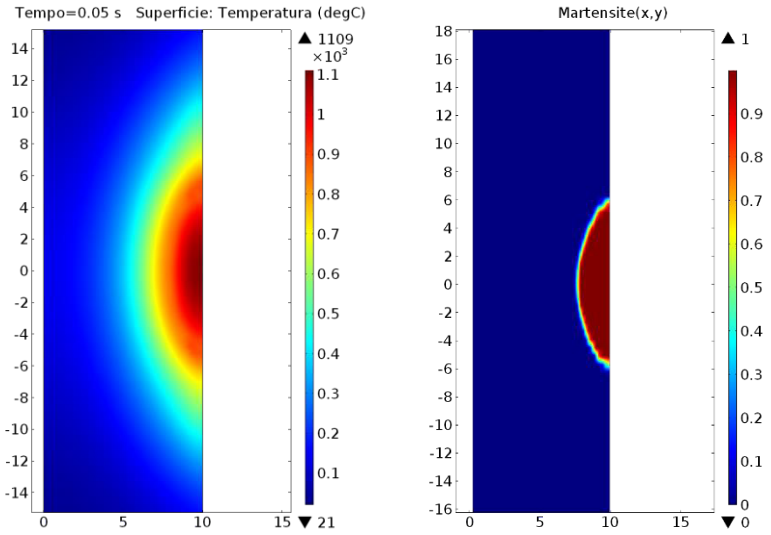

Figure 5: Temperature distriburion on the billet at the end of heating stage in the thermo-metallurgical simulation (left) and martensite distribution at the end of quenching (right)

5 CONCLUSIONS

A FEM based mathematical method has been developed in order to predict the phase transformations kinetics during the whole process of induction hardening. In particular:

- A non-linear magnetic behavior has been considered for the given steel, taking into account both magnetic saturation and Curie temperature.
- Both heating and quenching process have been simulated, calculating the complete thermal history and the microstructure at every time step that discretizes the process time.
- Different physical models have been weakly coupled in order to properly take into account the mutual dependences of material properties.

REFERENCES

[1] Dughiero, F., Forzan, M., Garbin, M., Pozza, C. and Sieni. E. A 3D numerical FEM model for the simualtion of induction welding of tubes, *COMPEL – The international journal for computation and mathematics in electrical and electronic engineering* (2011) **30**:1570-1581

[2] Dughiero, F., Forzan, M., Pozza. C. and Sieni, E., A Traslational Coupled Electromagnetic and Thermal Innovative Model for Induction Welding of Tubes, *IEEE Transaction on Magnetics* (2012) **48**:483-486

[3] Canova, A., Dughiero, F., Fasolo, F., Forzan, M., Freschi, F., Giaccone, L. and Repetto, M., Simplified approach for 3-D nonlinear induction heating problems, *IEEE Transaction on Magnetics* (2009) **45**:1855-1858

[4] Di Barba, P., Dughiero, F., Forzan, M. and Sieni, E., A Paretian Approach to Optimal Design with Uncertainties: Application in Induction Heating, *IEEE Transaction on Magnetics* (2014) **50**

[5] Schwenk, M., Hoffmeister, J. and Schulze, V. Experimental Determination of Process Parameters and Material data for Numerical Modeling of Induction Hardening, *Journal of Materials Engineering and Performance* (2013) **22**:1861-1870

[6] Nacke, B. and Wrona, E. Design of complex induction hardening problems by means of numerical simulation, *Archives of Electrical Engineering* (2005) **214**:461-466

[7] Candeo, A., Ducassy, C., Bocher, P. and Dughiero, F. Multiphysical modeling of induction hardening of ring gears for the aerospace industry, *IEEE Transaction on Magnetics* (2011) **47**:918-921

[8] Simsir, C. and Gür, C. H. A FEM based framework for simualtion of thermal treatments: Application to steel quenching, *Computational Materials Science* (2008) **44**:588-600

[9] Simsir, C. and Gür, C. H. 3D FEM simulation of steel quenching and investigation of the effect of asymmetric geometry on residual stress distribution, *Journal of Materials Processing Technology* (2008) **207**:211-221

[10] Lee, S. J., Matlock, D. K. and Van Tyne, C. J. Comparison of two finite element simulation codes used to model the carburizing of steel, *Computational Materials Science* (2013) **68**:47-54

[11] Leblond, J.B., Mottet, G., Devaux, J. and Devaux, J.C. Mathematical models of anisothermal phase transformations in steels, and predicted plastic behaviour, *Materials Science and Technology* (1985) **1**:815-822
[12] Kang, S.H. and Im, Y.T. Finite Element Investigation of Multi-Phase Transformation within Carburized Carbon Steel, *Journal of Materials Processing Technology* (2007) **183**:241-248
[13] Denis, S. Sjöström, S. and Simon, A. Coupled Temperature, Stress, Phase Transformation Calculation Model Numerical Illustration of the Internal Stresses Evolution during Cooling of a Eutectoid Carbon Steel Cylinder, *Metallurgical Transaction A* (1987) **18A**:1203-1212
[14] Haidemenopoulos, G. N. Coupled thermodynamic/kinetic analysis of diffusional transformations during laser hardening and laser welding, *Journal of Alloy and Compounds* (2001) **320**:302-307
[15] Dai, H. Modelling Residual Stress and Phase Transformations in Steel Welds, *Neutron Diffraction - Intech* (2012)
[16] Ferro, P. The use of Matlab in Advanced Design of Bonded and Welded Joints, *Application of MATLAB in Science and Engineering – Intech* (2011)
[17] Birò, O., Preis, K., Renhart, W., Vrisk, G. and Richter, K. R. Computation of 3D current driven skin effect problems using a current vector potential, *IEEE Transaction an Magnetics* (1993) **29**:1325-1328
[18] Orlich, J., Rose, A. and Wiest, P. *Atlas zur Wärmebehandlung der Stähle*, Vol. 3, Zeit-Temperatur-Austenitisierung-Schaubilder, Verlag Stahleisen, (1973)
[19] Kirkaldy, J. S. and Venugopalan, D. *Phase Transformations in Ferrous Alloys*, D.A.R. Marder and J.I. Goldstein, eds., AIME (1983)
[20] Victor Li, M., Niebuhr, V., Meekisho, L.L. and Atteridge D. G. A Computational Model for the Prediction of Steel Hardenability, *Metallurgical and Materials Transactions B* (1998) **29B**:661-672
[21] Zener, C. *Trans. AIME* (1946) **167**:550-83.
[22] Hillert, M. *Jernkont. Ann.*, (1957) **141**, 557-85.
[23] Koistinen, D. P. and Marburger, R. E. A General Equation Prescribing the Extent of the Austenite-Martensite Transformation in Pure Iron-Carbon Alloys and Plain Carbon Steels, *Acta Metallurgica* (1959) **7**:59-60
[24] Flux User Guide, www.cedrat.com